学位論文

Phenotypic Characterization and Clinical Outcome in Ampullary Adenocarcinoma

香川大学大学院医学系研究科

機能構築医学　専攻

浅野　栄介

Journal of Surgical Oncology

Phenotypic Characterization and Clinical Outcome in Ampullary Adenocarcinoma

Journal:	*Journal of Surgical Oncology*
Manuscript ID	JSO-2016-0120.R1
Wiley - Manuscript type:	Research Article
Date Submitted by the Author:	n/a
Complete List of Authors:	Asano, Eisuke ; Kagawa University, Gastroenterological Surgery Okano, Keiichi; Kagawa University, Gastroenterological Surgery Oshima, Minoru ; Kagawa University, Gastroenterological Surgery Kagawa, Seiko ; Kagawa University, Pathology Kushida, Yoshio ; Kagawa University, Pathology Munekage, Masaya; Kochi University School of Medicine Hanazaki, Kazuhiro; Kochi University School of Medicine Watanabe, Jota; Ehime University Graduate School of Medicine Takada, Yasutsugu ; Ehime University Graduate School of Medicine, Department of Hepato-Biliary-Pancreatic and Brest Surgery Ikemoto, Tetsuya; Tokushima University, Department of Digestive and Transplant Surgery Shimada, Mitsuo ; Tokushima University, Department of Digestive and Transplant Surgery Suzuki, Yasuyuki ; Kagawa University, Gastroenterological Surgery
Key Words:	ampullary adenocarcinoma, β-catenin, p53, pathologic subtype, mixed type

Research article

Phenotypic Characterization and Clinical Outcome in Ampullary Adenocarcinoma

Eisuke Asano, MD[1]; Keiichi Okano, MD, PhD [1]; Minoru Oshima, MD, PhD [1]; Seiko Kagawa, MD[2]; Yoshio Kushida, MD, PhD [2]; Masaya Munekage, MD, PhD [3]; Kazuhiro Hanazaki, MD, PhD [3]; Jota Watanabe, MD, PhD [4]; Yasutsugu Takada, MD, PhD [4]; Tetsuya Ikemoto, MD, PhD [5]; Mitsuo Shimada, MD, PhD [5]; Yasuyuki Suzuki, MD, PhD [1], On behalf of the Shikoku Consortium of Surgical Research (SCSR)

Departments of [1]Gastroenterological Surgery and [2]Pathology, Faculty of Medicine, Kagawa University, Kagawa, Japan

[3]Departments of First Surgery, Kochi University School of Medicine, Kochi, Japan

[4]Department of Hepato-Biliary-Pancreatic and Brest Surgery, Ehime University Graduate School of Medicine, Ehime, Japan

[5]Department of Digestive and Transplant Surgery, Tokushima University, Tokushima, Japan

Address Correspondence to:

Keiichi Okano, MD, PhD, FACS

Department of Gastroenterological Surgery, Faculty of Medicine, Kagawa University

1750-1 Ikenobe, Miki-cho, Kita-gun, Kagawa 761-0793, Japan

E-mail: kokano@med.kagawa-u.ac.jp Fax: +81 (87) 891-2439 Tel: +81 (87) 891-2438

Financial Support: Supported by a Grant-in-Aid for Scientific Research (25462115) from the Ministry of Education, Science and Culture of Japan.

The authors have no financial conflicts of interest related to this work.

Running title: Characterization of Ampullary cancer

Category: Research article

Total number of each: 2492 words in Text, 3 tables, 7 Figures, 1 supplementary table, 1 supplementary figure

Key words: ampullary adenocarcinoma, *β-catenin,* p53, pathologic subtype, mixed type

Synopsis: Expression of MUC1, MUC2, p53 and *KRAS* mutation in ampullary adenocarcinoma have an impact on clinical consequence. The mixed subtype may have a distinct tumor nature as compared to the intestinal and pancreatobiliary subtypes.

ABSTRACT

Background. Although various features of ampullary adenocarcinoma have been reported, the impact of genetic alterations and rare subtypes on clinical outcome remains unclear.

Methods. We determined the expression of proteins, including MUC1, MUC2, p53, p16, Smad/Dpc4 and β-catenin, and genetic mutations such as *KRAS, BRAF,* and *GNAS* mutations in 69 patients with ampullary adenocarcinoma to clarify their relationships with clinicopathological findings and subtypes.

Results. Kaplan-Meier survival analysis indicated that abnormal p53 labeling was significantly associated with a shorter overall survival. MUC1-positive and MUC2-negative expressions were significantly associated with lymphatic invasion, pancreatic invasion, lymph node metastasis, and advanced UICC Stage. The *KRAS* mutation was significantly associated with large tumor size and pancreatic invasion. There were 35 intestinal (50%), 15 pancreatobiliary (22%), and 11 the mixed subtype (16%) tumors. Patients with the mixed subtype showed significantly poor outcome. The invasiveness of the mixed subtype was similar to that of the pancreatobiliary subtype;

moreover, the mixed subtype showed a high incidence of abnormal β-catenin immunolabeling (73%).

Conclusions. Protein expression and genetic mutation are clinically associated with the characteristics of ampullary adenocarcinoma. The mixed subtype may have a distinct tumor nature as compared to other 2 major subtypes.

INTRODUCTION

Although ampullary adenocarcinoma is a relatively uncommon disease, and accounts for 0.2–0.5% of gastrointestinal malignancies, the rate of ampullary cancer has been increasing annually over the last few years.[1 2 3] The varying prognosis of patients with ampullary adenocarcinoma weakens the interpretation of clinical trials and hampers clinical decision making.[2, 4, 5] One of the reasons for such difficulty in interpretation may that the tumors arise from any one of 3 epithelia (duodenal, biliary, or pancreatic) that converge at this location.[6]

Based on the epithelium from which the adenocarcinoma originates, ampullary adenocarcinoma can be classified into 2 subgroups: the intestinal type and pancreatobiliary type.[7 8-15] The intestinal-type adenocarcinomas originate from the intestinal epithelium overlying the ampulla and evolve through an adenoma-carcinoma sequence.[16, 17] The pancreatobiliary-type adenocarcinomas originate from the endothelium of the distal common bile duct, pancreatic duct, or common ampullary channel, and arise from precursor large-duct pancreatic intraepithelial neoplasia.[8-10] In a previous study, we have described the clinical significance of the 2 major pathological

subtypes and other prognostic factors of this disease.[18, 19] The patients with the pancreatobiliary type have consistently been shown to have worse prognoses. However, the immunohistochemical (IHC) and genetic features of these subtypes remain unclear. In addition, another type of tumor was detected that contains both the components of the intestinal and pancreatobiliary type. Hence, further research on the pathogenesis and biology of these subtypes of ampullary cancer could clarify the treatment strategy for this disease.

In the present study, we aimed to assess the clinicopathological features, prognosis, and histological subtypes of ampullary cancer via a multi-institutional study in the Shikoku Consortium of Surgical Research (SCSR), Japan. In particular, we evaluated the genetic and IHC markers associated with the different histological types including the mixed type and the associated prognosis.

PATIENTS AND METHODS

We reviewed the findings of 69 patients who received curative resection for ampullary adenocarcinoma at 4 university hospitals affiliated with the SCSR between January 1985 and December 2012. The paraffin blocks of specimens from these 69

patients were prospectively prepared for pathologic, IHC, and genetic studies at Kagawa University. This study was approved by the Kagawa University and each center review board. Tumors were staged in accordance with the 7th edition of the TNM staging system for ampullary carcinoma issued by the American Joint Committee on Cancer.[20]

Pathological review

Tissue samples were first examined using hematoxylin-eosin stained sections. The histological subtype of each tumor was re-evaluated by 2 pathologists (YK and SK) who were blinded to the clinical findings, based on the guidelines of Albores-Saavedra et al.[21] In brief, they separately assessed the proportion of each component (intestinal or pancreatobiliary features), and the histological subtype was classified according to the dominant component; however, the cases of mixed type were classified by both pathologists wherein both components comprised >20% of the sample area.

IHC review

All samples were stained immunohistochemically with the following antibodies: cytokeratin 20 (Ks20.8, diluted 1:75, Leica), cytokeratin 7 (OV-TL12/30, diluted 1:150, Leica), CDX2 (AMT28, diluted 1:50, Leica), MUC1 (Ma552, diluted 1:150, Leica),

MUC2 (Ccp 58, diluted 1:300, Leica), p53 (DO-7, diluted 1:9600, DAKO), p16 (E6H4, diluted 1:6, MTM laboratories), Smad/Dpc4 (B-8, diluted 1:200, Santa Cruz), and β-catenin (14/Beta-Catenin, diluted 1:1000, BD Biosciences). IHC staining was performed with the Leica BOND III automatic immunostainer (Leica Microsystems) after incubation of the sample in a decloaking chamber for antigen activation. IHC analysis was performed by 2 surgeons (EA and MO). IHC staining was scored according to the percentage of tumor cells that were stained. We arbitrarily defined IHC positivity as a condition wherein >30% of the tumor cells were positively stained.[22] However, p53 immunolabeling was classified as follows: normal, wherein 5–30% of tumor cells were stained positively on p53 immunolabeling; and abnormal, wherein <5% of tumor cells were stained positively on p53 immunolabeling (suggesting the presence of an intragenic deletion, nonsense mutation, or >30% of tumor cells were stained positively on p53 immunolabeling (suggesting the presence of a missense mutation).[23] The β-catenin expression was classified according to the membranous staining of the tumor cells; if >50% of tumor cells were stained positively, we considered that the expression of β-catenin was normal.

DNA sequence analysis

One hematoxylin and eosin-stained slide and 5–10 subsequent unstained 4-μm sections were prepared from paraffin-embedded tissue samples. With regard to the hematoxylin and eosin-stained slide, the sample was macrodissected using a razor, deparaffinized in xylene, and rehydrated with ethanol. Tumor DNA was extracted using a QIAamp DNA FFPE Tissue Kit (#56404, Qiagen) according to the manufacturer's protocol. The DNA alterations were verified by Sanger sequencing. Polymerase chain reaction (PCR) was performed using HotStar Taq DNA Polymerase (QIAGEN). A 20-μL volume for the PCR reaction contained 2 μL 10PCR Buffer, 0.5 μM of each primer, 20 ng/μL of template DNA, 0.5 U of HotStar Taq DNA Polymerase, 200 μM of each dNTP, and sterile distilled water. The PCR products containing codon 12 and 13 of *KRAS*, codon 600 of *BRAF*, and codon 201 of *GNAS* were amplified using the primers. The sequencing results were compared with the corresponding entries in the Ensembl database (*KRAS*: ENST00000311936, *BRAF*: ENST00000288602, *GNAS*: ENST00000371085).

Statistical analysis

All statistical analyses were performed using JMP11 (SAS Institute Inc., Cary, NC, USA). The different clinicopathologic parameters were used as variables in the chi-square test or Fisher's exact test. Survival curves were estimated using the Kaplan-Meier method, and differences in survival were compared using the log rank test. We considered a P value of <0.05 to indicate statistical significance.

RESULTS

Clinicopathologic characteristics and outcome

The median age at operation was 68.0 years (range, 46–84 years), whereas the median follow-up duration of the patients was 30 months (range, 0–252 months). The cohort of 69 patients (**Table 1**) consisted of 26 women (37.7%) and 43 men (62.3%). The 1-, 3-, and 5-year survival rates were 89.1%, 68.8%, and 52.8%, respectively. Of the 69 re-evaluated tumors, 35 were intestinal (50.7%), 15 were pancreatobiliary (21.7%), and 11 were of the mixed subtype (15.9%); of the other 8 tumors, 3 cases were poorly differentiated but could not be classified, and the 2 pathologists could not reach a consensus regarding the remaining 5 tumors, were excluded subtype analysis.

The IHC results are also shown in **Table 1** and **Figure 1-6**. Abnormal p53

immunolabeling was detected in 56 (82.4%) of the 69 patients. Twenty-eight (41.2%) tumors showed a lack of p53 immunolabeling as compared to the adjacent normal tissue (immunolabeling in <5% of neoplastic cells) (**Figure 1b**) and 28 (41.2%) tumors showed robust nuclear accumulation of immunolabeled p53 in ≥30% of the neoplastic cells as compared to the adjacent normal cells (**Figure 1c**). Loss of or weak β-catenin immunolabeling was observed in 28 (41.8%) of 69 patients. On sequence analysis, the *KRAS* gene mutation was detected in 26 cases (39.4%) and the *BRAF* gene mutation was detected in 2 cases (3.0%), but no *GNAS* gene mutation was detected. An activating *KRAS* gene mutation was identified in 26 of 66 cases of ampullary adenocarcinoma (39.4%). With regard to the amino acid change caused by the *KRAS* mutation, G12D was detected in 11 cases; G12V was detected in 8 cases; G13D was detected in 3 cases; and G12C, G12S, G12A, and G12D+G13D were detected in 1 case each (**Supplementary figure**).

Kaplan-Meier survival analysis (**Table 1)** indicated that subtype ($P = 0.0007$) (**Figure 7a**), pathological grade ($P = 0.0012$) (**Figure 7b**), lymphatic invasion ($P = 0.0015$), vascular invasion ($P = 0.0255$), perineural invasion ($P = 0.0080$), pancreatic

invasion ($P = 0.0002$), duodenal invasion ($P = 0.0010$), lymph node metastasis ($P = 0.0040$) **(Figure 7c)**, and abnormal p53 labeling ($P = 0.0137$) **(Figure 7d)** were significantly associated with shorter overall survival. Multivariate models using Cox proportional hazards analysis included parameters that were significant ($P < 0.05$) on univariate analysis with log-rank tests. No significant difference was observed among these parameters on multivariate analysis.

Association between protein expression/genetic mutation and clinicopathologic factors

Table 2 summarizes the relationships among CK20, CK7, CDX2, MUC1, MUC2, p16, p53, and Smad4/Dpc4 positivity; β-catenin immunolabeling; *KRAS* mutation; *BRAF* mutation; and clinicopathologic parameters (**details in supplementary table**). MUC1 positivity was significantly associated with tumor differentiation ($P < 0.0001$), lymphatic invasion ($P = 0.0028$), duodenal invasion ($P = 0.0195$), pancreatic invasion ($P = 0.0309$), lymph node metastasis ($P = 0.0016$), and the tumor stage ($P = 0.0044$). MUC2 positivity was significantly associated with lymphatic invasion ($P = 0.0004$), perineural invasion ($P = 0.0242$), pancreatic invasion ($P = 0.0162$), and lymph

node metastasis ($P = 0.0162$). The loss of p16 immunolabeling was significantly ($P = 0.0044$) associated with smaller tumor size (< 20 mm). Moreover, the *KRAS* mutation was significantly associated with tumor size ($P = 0.0142$) and pancreatic invasion ($P = 0.043$). Abnormal β-catenin immunolabeling was significantly associated with the pathological grade ($P = 0.0333$).

Correlation between pathologic subtype and clinicopathologic factors/histomolecular phenotype

Table 3 summarizes the relationships between the histological subtype and clinicopathological or molecular biological parameters. There was a significant difference in pathological grade ($P = 0.0139$), lymphatic invasion ($P = 0.0093$), perineural invasion ($P = 0.04$), pancreatic invasion ($P = 0.0037$), duodenal invasion ($P = 0.0368$), lymph node metastasis ($P = 0.0037$), tumor stage ($P = 0.0307$), CK20 positivity ($P = 0.0017$), MUC1 positivity ($P = 0.0064$), and β-catenin immunolabeling ($P = 0.0347$) among 3 histological subtypes. Pancreatobiliary and mixed adenocarcinoma were significantly associated with pathological invasiveness (lymphatic, perineural, pancreatic, and duodenal) or lymph node metastases. The mixed subtype was associated with a high incidence of abnormal β-catenin

immunolabeling (73%) as compared to the intestinal type (30%), and was also associated with a poorer survival.

DISCUSSION

The common immunohistochemical markers for ampullary adenocarcinoma include cytokeratin 20, cytokeratin 7, CDX2, MUC1, and MUC2, which are often used for discrimination between the subtypes.[10, 24-27] These markers did not show a significant impact on survival in the present study. In fact, only p53 had a significant impact on survival. In particular, MUC1 positivity and MUC2 negativity were associated with pathological invasiveness and lymph node metastasis. In addition to cytokeratin 20, cytokeratin 7, CDX2, MUC1, and MUC2, the present results suggested that p53, β-catenin, and p16 were also significant IHC makers for determining prognosis or clinicopathologic characteristics in patients with ampullary adenocarcinoma.

The *KRAS* mutation was detected in 26 of 66 patients (39.4%) in the present study, including 11 (48%) cases with the intestinal type, 7 (30%) with the pancreatobiliary type, and 5 (21%) with the mixed type. The *KRAS* mutation was found

to be associated with pancreatic invasion and large size of the tumor. Three research groups have reported on the prevalence rates of *KRAS* mutations in their series of ampullary adenocarcinoma (44%, 28.6%, and 23%).[28-30] Given the similar prevalence of *KRAS* mutations in colon cancer,[31] we believe that patients with wild-type *KRAS* may be candidates for treatment with epidermal growth factor receptor-targeted therapy with cetuximab or panitumumab.

Albores-Saavedra et al[21] introduced a histologic classification system for these tumors; accordingly, the tumors were classified as pancreatobiliary, intestinal, mixed, mucinous, poorly differentiated, and invasive papillary types. Our retrospective investigation confirmed the applicability of this classification system as well as the histologic variability of ampullary adenocarcinomas; in fact, the diagnoses of the 2 pathologists were concordant in 93% of the cases. In the remaining cases, classification was difficult as these tumors often showed a greater variability in the phenotype. The prevalence of the different subtypes observed in our series is also consistent with the observations from other studies. The overall prevalence of the intestinal type ranged from 27% to 49%, whereas that of the pancreatobiliary type ranged from 21% to 45%.[21,

[22] Only limited information was available on the other types of ampullary adenocarcinomas. Kohler et al[30] found 6 mixed (8%), 3 poorly differentiated (4%), and 4 mucinous (6%) carcinomas among 71 patients with ampullary adenocarcinoma. The most recent and largest investigation including 3 different cohorts identified 5 (7%), 5 (6%), and 4 (9%) cases of mixed adenocarcinoma from 72, 90, and 46 periampullary carcinomas, respectively.[32] In the present study, we observed 11 cases of mixed (16%) from 69 patients with ampullary adenocarcinoma. No consensus was reached regarding the frequency and characteristics of the mixed or minor phenotypes, except for the pancreatobiliary and intestinal phenotypes.

Furthermore, there is no clear definition regarding the mixed subtype comprising both the pancreatobiliary and intestinal phenotypes. Chang et al.[13] defined the mixed type (6–9%) as the tumor that contained ≥10% of both histologic types. In contrast, Ang et.al.[22] defined mixed subtype as a tumor that comprised ≥25% of both histologic types or tumors that were entirely composed of hybrid patterns. The authors had classified 13 of the 105 patients (12%) as having the mixed subtype. Interestingly, excellent interobserver agreement was observed for the poorly differentiated and mucinous

subtypes, only good interobserver agreement was noted for the intestinal and pancreatobiliary subtypes, and poor interobserver agreement was observed for the mixed subtype on hematoxylin and eosin evaluation. The authors concluded that IHC evaluation, in combination with HE evaluation, enhanced the subtyping of ampullary adenocarcinoma, including the mixed subtype.

Only few studies have described the prognosis and characteristics of mixed type adenocarcinoma. Chang et al[32] reported on the intermediate prognosis of the mixed type of the pancreatobiliary and intestinal phenotypes. The present study indicated that the pathological characteristics of the mixed type were similar to those of the pancreatobiliary type, and that the prognosis of the mixed type was poor in comparison to that of the intestinal phenotype. The tumor heterogeneity of the mixed phenotype may be one explanation for the resistance to the treatment. Hence, future studies should also consider this diversity when assessing these types of tumors.

It is interesting to note that a mixed immunophenotype expressed abnormal membranous β-catenin in 8 of 11 patients (72%), whereas the abnormal β-catenin expression rates were 30% in the intestinal and 53% in the pancreatobiliary subtype.

Hsu et al[33] found that the loss of membranous β-catenin expression was associated with tumor markers, ulcerative type, liver metastases, and poor prognosis. The Wnt/β-catenin signaling pathway is a critical pathway in gastrointestinal tumor genesis, particularly in cases of colorectal cancer.[34] Hence, the involvement of multiple mechanisms in the carcinogenesis and regulation of β-catenin in ampullary neoplasms could potentially explain the nature of the mixed subtype. The other rare subtypes including poorly differentiated type require further investigation in large case series, as there are very few cases in this study.

Our study provides further evidence that ampullary adenocarcinomas are a heterogeneous group of cancers that differ according to conventional histologic features, immunophenotype (MUC1, MUC2, p16, p53, and β-catenin), and *KRAS* genotype. These differences could influence patient prognosis or tumor nature. The present study indicated that the histomolecular phenotype is not only valuable for predicting the prognosis of patients, but could have an impact on treatment. Future studies targeting appropriate phenotype would be required for selecting ideal candidate for adjuvant

therapy. The results suggest that these tumors require highly personalized clinical approach according to their tumor nature.

Acknowledgements

We acknowledge Shinichi Yachida MD PhD for inspiring this study.

REFERENCES

1. Kim RD, Kundhal PS, McGilvray ID, et al. Predictors of failure after pancreaticoduodenectomy for ampullary carcinoma. *J Am Coll Surg* 2006; 202(1):112-9.

2. Howe JR, Klimstra DS, Moccia RD, et al. Factors predictive of survival in ampullary carcinoma. *Ann Surg* 1998; 228(1):87-94.

3. Fischer H-P, Zhou H. Pathogenesis of carcinoma of the papilla of Vater. *Journal of Hepato-Biliary-Pancreatic Surgery* 2004; 11(5):301-309.

4. Talamini MA, Moesinger RC, Pitt HA, et al. Adenocarcinoma of the ampulla of Vater. A 28-year experience. *Ann Surg* 1997; 225(5):590-9; discussion 599-600.

5. Monson JT, Donohue JH, McEntee GP, et al. Radical resection for carcinoma of

the ampulla of vater. *Archives of Surgery* 1991; 126(3):353-357.

6. Sarmiento JM, Nagomey DM, Sarr MG, et al. Periampullary cancers: are there differences? *Surg Clin North Am* 2001; 81(3):543-55.

7. Kimura W, Ohtsubo K. Incidence, sites of origin, and immunohistochemical and histochemical characteristics of atypical epithelium and minute carcinoma of the papilla of Vater. *Cancer* 1988; 61(7):1394-402.

8. Kimura W, Futakawa N, Yamagata S, et al. Different clinicopathologic findings in two histologic types of carcinoma of papilla of Vater. *Jpn J Cancer Res* 1994; 85(2):161-6.

9. Kimura W, Futakawa N, Zhao B. Neoplastic diseases of the papilla of Vater. *J Hepatobiliary Pancreat Surg* 2004; 11(4):223-31.

10. Zhou H, Schaefer N, Wolff M, et al. Carcinoma of the ampulla of Vater: comparative histologic/immunohistochemical classification and follow-up. *Am J Surg Pathol* 2004; 28(7):875-82.

11. Albores-Saavedra J HD, Klimstra DS. Tumors of the gallbladder, extrahepatic bile ducts, and ampulla of Vater. In: Rosai J, Sobin L, editors: . *Tumor Pathology.*

Third series, Fascicle 27. Washington DC: Armed Forces Institute of Pathology 2000:pp. 259–316.

12. Agoff SN, Crispin DA, Bronner MP, et al. Neoplasms of the ampulla of vater with concurrent pancreatic intraductal neoplasia: a histological and molecular study. *Mod Pathol* 2001; 14(3):139-46.

13. Chang DK, Jamieson NB, Johns AL, et al. Histomolecular phenotypes and outcome in adenocarcinoma of the ampulla of vater. *J Clin Oncol* 2013; 31(10):1348-56.

14. Winter JM, Cameron JL, Campbell KA, et al. 1423 pancreaticoduodenectomies for pancreatic cancer: A single-institution experience. *J Gastrointest Surg* 2006; 10(9):1199-210; discussion 1210-1.

15. Westgaard A, Pomianowska E, Clausen OP, et al. Intestinal-type and pancreatobiliary-type adenocarcinomas: how does ampullary carcinoma differ from other periampullary malignancies? *Ann Surg Oncol* 2013; 20(2):430-9.

16. Baczako K, Buchler M, Beger HG, et al. Morphogenesis and possible precursor lesions of invasive carcinoma of the papilla of Vater: epithelial dysplasia and

adenoma. *Hum Pathol* 1985; 16(3):305-10.

17. Kozuka S, Tsubone M, Yamaguchi A, et al. Adenomatous residue in cancerous papilla of Vater. *Gut* 1981; 22(12):1031-4.

18. Okano K, Oshima M, Yachida S, et al. Factors predicting survival and pathological subtype in patients with ampullary adenocarcinoma. *J Surg Oncol* 2014.

19. Okano K, Asano E, Kushida Y, et al. Factors influencing lymph node metastasis in patients with ampullary adenocarcinoma. *Dig Surg* 2014; 31(6):459-67.

20. Edge S, Byrd DR, Compton CC, et al. AJCC Cancer Staging Manual. 7 ed: Springer New York, 2010.

21. Albores-Saavedra J, Henson DE, Klimstra DS. Tumors of the gallbladder, extrahepatic bile ducts, and ampulla of Vater.: Armed Forces Institute of Pathology,,Washington,D.C., 2000.

22. Ang DC, Shia J, Tang LH, et al. The utility of immunohistochemistry in subtyping adenocarcinoma of the ampulla of vater. *Am J Surg Pathol* 2014; 38(10):1371-9.

23. Oshima M, Okano K, Muraki S, et al. Immunohistochemically detected expression of 3 major genes (CDKN2A/p16, TP53, and SMAD4/DPC4) strongly predicts survival in patients with resectable pancreatic cancer. *Ann Surg* 2013; 258(2):336-46.

24. Westgaard A, Schjolberg AR, Cvancarova M, et al. Differentiation markers in pancreatic head adenocarcinomas: MUC1 and MUC4 expression indicates poor prognosis in pancreatobiliary differentiated tumours. *Histopathology* 2009; 54(3):337-47.

25. de Paiva Haddad LB, Patzina RA, Penteado S, et al. Lymph node involvement and not the histophatologic subtype is correlated with outcome after resection of adenocarcinoma of the ampulla of vater. *J Gastrointest Surg* 2010; 14(4):719-28.

26. Matsubayashi H, Watanabe H, Yamaguchi T, et al. Differences in mucus and K-ras mutation in relation to phenotypes of tumors of the papilla of vater. *Cancer* 1999; 86(4):596-607.

27. Chu PG, Schwarz RE, Lau SK, et al. Immunohistochemical staining in the diagnosis of pancreatobiliary and ampulla of Vater adenocarcinoma: application

of CDX2, CK17, MUC1, and MUC2. *Am J Surg Pathol* 2005; 29(3):359-67.

28. Wagner PL, Chen YT, Yantiss RK. Immunohistochemical and molecular features of sporadic and FAP-associated duodenal adenomas of the ampullary and nonampullary mucosa. *Am J Surg Pathol* 2008; 32(9):1388-95.

29. Schonleben F, Qiu W, Allendorf JD, et al. Molecular analysis of PIK3CA, BRAF, and RAS oncogenes in periampullary and ampullary adenomas and carcinomas. *J Gastrointest Surg* 2009; 13(8):1510-6.

30. Kohler I, Jacob D, Budzies J, et al. Phenotypic and genotypic characterization of carcinomas of the papilla of Vater has prognostic and putative therapeutic implications. *Am J Clin Pathol* 2011; 135(2):202-11.

31. Lee DW, Kim KJ, Han SW, et al. KRAS mutation is associated with worse prognosis in stage III or high-risk stage II colon cancer patients treated with adjuvant FOLFOX. *Ann Surg Oncol* 2015; 22(1):187-94.

32. Chang DK, Jamieson NB, Johns AL, et al. Histomolecular Phenotypes and Outcome in Adenocarcinoma of the Ampulla of Vater. *Journal of Clinical Oncology* 2013; 31(10):1348-1356.

33. Hsu HP, Shan YS, Jin YT, et al. Loss of E-cadherin and beta-catenin is correlated with poor prognosis of ampullary neoplasms. *J Surg Oncol* 2010; 101(5):356-62.

34. Kolligs FT, Bommer G, ouml, et al. Wnt/Beta-Catenin/Tcf Signaling: A Critical Pathway in Gastrointestinal Tumorigenesis. *Digestion* 2002; 66(3):131-144.

FIGURE LEGENDS

Figure 1

Typical immunohistochemical labeling profiles of p53 in ampullary adenocarcinoma (×100 magnification, lower right×400 magnification). **a**. (5-30%), Example of normal pattern of ampullary adenocarcinoma for p53. Positive nuclear labeling is present in scattered cells of the neoplastic glands. **b**. (<5%, loss), Example of abnormal pattern for p53 (loss type). Nuclear labeling is absent in almost every cell of the neoplastic glands. **c**. (30%<, diffuse), Example of abnormal pattern of p53 (diffuse type). Diffusely positive nuclear labeling is present in the neoplastic glands.

Figure 2

Typical immunohistochemical labeling profiles of p16 in ampullary adenocarcinoma (×100 magnification, lower right×400 magnification). **a**. Example of negative pattern of ampullary adenocarcinoma for p16. Positive labeling is absent in the neoplastic glands. In contrast, positive labeling is seen within adjacent normal cells (*). **b**. Example of positive pattern for p16. Positive nuclear and cytoplasmic labeling is present in the neoplastic glands.

Figure 3

Typical immunohistochemical labeling profiles of Smad4/Dpc4 in ampullary adenocarcinoma (×100 magnification, lower right×400 magnification). **a**. Example of negative pattern of ampullary adenocarcinoma for Smad4/Dpc4. Nuclear and cytoplasmic labeling is absent in the neoplastic glands. In contrast, positive labeling is seen in adjacent stromal cells. **b**. Example of positive pattern for Smad4/Dpc4. Positive nuclear and cytoplasmic labeling is present in the neoplastic glands.

Figure 4

Typical immunohistochemical labeling profiles of β-catenin in ampullary adenocarcinoma (×100 magnification, lower right×400 magnification). a. Example

of normal pattern of ampullary adenocarcinoma for β-catenin. Membrane labeling is stronger than nuclear or cytoplasmic labeling in the neoplastic glands. b. Example of loss pattern for β-catenin. Membrane labeling is weak, and positive nuclear or cytoplasmic labeling is present in the neoplastic glands. In contrast, positive membrane labeling is seen in the adjacent normal duodenal glands (N).

Figure 5

Typical immunohistochemical labeling profiles of MUC1 in ampullary adenocarcinoma (×100 magnification, lower right×400 magnification). a. Example of negative pattern of ampullary adenocarcinoma for MUC1. Positive labeling is absent in the neoplastic glands. In contrast, positive labeling is seen within adjacent normal pancreatic ductal cells (N). b. Example of positive pattern for MUC1. Positive labeling is present in the cytoplasm and membrane of the neoplastic glands.

Figure 6

Typical immunohistochemical labeling profiles of MUC2 in ampullary adenocarcinoma (×100 magnification, lower right×400 magnification). a. Example of negative pattern of ampullary adenocarcinoma for MUC2. Positive labeling is

absent in the neoplastic glands. In contrast, positive labeling is seen in the goblet cells of adjacent normal duodenal glands (N). b. Example of positive pattern for MUC2. Positive labeling is present in the cytoplasm of the neoplastic glands.

Figure 7

Kaplan-Meier curve of patients with ampullary adenocarcinoma who underwent curative surgery according to the pathologic or immunohistochemical analysis.

a. Subtypes, **b.** Pathological grade, **c.** Lymph node metastasis, **d.** p53 immunolabeling. The short crossed lines represent the censored cases.

Supplementary Figure

Sequencing analysis of *KRAS* in ampullary adenocarcinoma.

An activating *KRAS* gene mutation was identified in 26 of 66 cases of ampullary adenocarcinoma (39.4%). With regard to the amino acid change caused by the *KRAS* mutation, G12D was detected in 11 cases; G12V was detected in 8 cases; G13D was detected in 3 cases; and G12C, G12S, G12A, and G12D+G13D were detected in 1 case each.

Table 1. Clinicopathologic parameters and outcome (n = 69)

Variable	No. of patients (%)	Overall survival (%)		
		3 years	5 years	Log-rank (*P* value)
Overall	69 (100)	68.6	52.8	
Gender				
Female	26 (37.7)	68.5	46.9	0.5353
Male	43 (62.3)	69.8	56.1	
Tumor size, mm				
Mean	20.3 (SD, 11.0)			
Median (Range)	19.0 (5 – 70)			
≤ 20 mm	43 (62.3)	71.7	62.7	0.2386
> 20 mm	26 (37.7)	64.4	34.5	
Pathological grade				
well	35 (50.7)	92.2	79.9	
moderately	26 (37.7)	37.5	28.1	0.0012
poor	6 (8.7)	53.3	26.7	
other	2 (2.9)			
Histological subtype				
Intestinal	35 (50.7)	95.5	70.7	
pancreatobiliary	15 (21.7)	63.9	53.3	0.0007
mixed	11 (15.9)	30.5	15.2	
other	8 (11.6)			
Lymphatic invasion				
Negative	22 (31.9)	100	83.3	0.0015
Positive	41 (59.4)	55.4	37.5	
Unknown	6 (8.7)			
Vascular invasion				
Negative	35 (50.7)	79.7	73.5	0.0255
Positive	28 (40.6)	61.9	34.4	
Unknown	6 (8.7)			
Perineural invasion				
Negative	39 (56.5)	79.8	58.4	0.0080
Positive	18 (26.1)	46.4	23.2	
Unknown	12 (17.4)			
Pancreatic invasion				
Negative	40 (58.0)	91.7	72.2	0.0002
Positive	29 (42.0)	41.2	29.4	
Duodenal invasion				
Negative	17 (24.6)	100	100	0.0010

Positive	52 (75.4)	55.8	35.9	
Lymph nodes metastasis				
Negative	40 (58.0)	88.3	64.6	0.0040
Positive	29 (42.0)	42.6	36.6	
Stage (UICC)				
IA	16 (23.2)	100	100	
IB	15 (21.7)	80.0	40.0	
IIA	6 (8.7)	100	66.7	0.0028
IIB	27 (39.1)	43.0	36.9	
III	2 (2.9)	50.0	0	
IV	3 (4.3)	33.3	0	
Immunohistochemistry				
CK20				
Negative	16 (23.5)	55.0	44.0	0.3234
Positive	52 (76.5)	77.3	57.9	
CK7				
Negative	9 (13.2)	58.3	58.3	0.7098
Positive	59 (86.8)	70.6	52.7	
CDX2				
Negative	42 (61.8)	65.4	53.3	0.7029
Positive	26 (38.2)	84.3	52.7	
MUC1				
Negative	40 (58.8)	82.5	57.7	0.3219
Positive	28 (41.2)	55.5	48.6	
MUC2				
Negative	57 (83.8)	67.6	50.5	0.2240
Positive	11 (16.2)	85.7	85.7	
p53				
abnormal	56 (82.4)	63.4	43.2	0.0137
normal	12 (17.6)	100	100	
p16				
Negative	30 (44.1)	69.1	50.3	0.6088
Positive	38 (55.9)	71.1	57.1	
SMAD4				
Negative	17 (25.0)	50.5	37.9	0.1291
Positive	51 (75.0)	77.6	59.9	
β-catenin (membrane)				
loss or weak	28 (41.8)	52.2	37.3	0.0585

normal	39 (58.2)	83.1	65.1	
DNA sequence				
KRAS				
WT	40 (60.6)	73.8	52.7	0.7935
mutation	26 (39.4)	65.9	53.9	
BRAF				
WT	65 (97.0)	72.2	55.4	0.3613
mutation	2 (3.0)	0	0	
GNAS				
WT	68 (100)	70.3	53.9	
mutation	0			

Abbreviations: SD, standard deviation; UICC, Union for International Cancer Control.

Table 2. Summary of significant association between phenotypes and clinicopathological parameters (n=69)

	n (%)	Clinicopathological Parameters	P value
Immunohistochemistry			
MUC1 positive	28 (41.2)	Moderately to poor pathological grade	<0.0001
		Lymphatic invasion	0.002
		Duodenal invasion	0.019
		Pancreatic invasion	0.03
		Lymph nodes metastasis	0.001
		Advanced stage (UICC)	0.004
MUC2 negative	57 (83.8)	Lymphatic invasion	0.0004
		Perineural invasion	0.024
		Pancreatic invasion	0.016
		Lymph nodes metastasis	0.016
		Advanced stage (UICC)	0.042
P53 abnormal	56 (82.4)	Duodenal invasion	0.03
P16 positive	38 (55.9)	Large tumor size (20mm<)	0.004
β-catenin negative	28 (41.8)	Moderately to poor pathological grade	0.033
DNA sequence			
KRAS mutation	26 (39.4)	Large tumor size (20mm<)	0.014
		Pancreatic invasion	0.043

Table 3. Relationship between histological subtype and Clinicopathological or molecular biological Parameters

	Histological subtype			P value
	Intestinal type (%)	Pancreatobiliary type (%)	Mixed type (%)	
Gender				
Female	11 (31)	7 (47)	4 (36)	0.5892
Male	24 (69)	8 (53)	7 (64)	
Tumor size, mm				
≤ 20 mm	21 (60)	11 (73)	6 (55)	0.5661
> 20 mm	14 (40)	4 (27)	5 (45)	
Pthological type				
well	24 (73)	4 (27)	3 (27)	0.0139
moderately	8 (24)	9 (60)	7 (64)	
poor	1 (3)	2 (13)	1 (9)	
Lymphatic invasion				
Negative	17 (53)	2 (15)	1 (10)	0.0093
Positive	15 (47)	11 (85)	9 (90)	
Vascular invasion				
Negative	21 (66)	6 (46)	5 (50)	0.4113
Positive	11 (34)	7 (54)	5 (50)	
Perineural invasion				
Negative	22 (79)	4 (36)	7 (70)	0.0400
Positive	6 (21)	7 (64)	3 (30)	
Pancreatic invasion				
Negative	27 (77)	5 (33)	4 (36)	0.0037
Positive	8 (23)	10 (67)	7 (64)	
Duodenal invasion				
Negative	12 (34)	2 (13)	0 (0)	0.0368
Positive	23 (66)	13 (87)	11 (100)	
Lymph nodes metastasis				
Negative	27 (77)	5 (33)	4 (36)	0.0037
Positive	8 (23)	10 (67)	7 (64)	
Stage (UICC)				
IA	11 (31)	2 (13)	0 (0)	0.0307
IB	11 (31)	2 (13)	2 (18)	
IIA	5 (14)	0 (0)	1 (9)	

IIB	8 (23)	9 (60)	7 (64)	
LII	0 (0)	1 (7)	0 (0)	
IV	0 (0)	1 (7)	1 (9)	
Immunohistochemistry				
CK20				
Negative	2 (6)	5 (33)	6 (55)	0.0017
Positive	31 (94)	10 (67)	5 (45)	
CK7				
Negative	4 (12)	1 (7)	2 (18)	0.6672
Positive	29 (88)	14 (93)	9 (82)	
CDX2				
Negative	16 (48)	11 (73)	8 (73)	0.1616
Positive	17 (52)	4 (27)	3 (27)	
MUC1				
Negative	25 (76)	5 (33)	4 (36)	0.0064
Positive	8 (24)	10 (67)	7 (64)	
MUC2				
Negative	24 (73)	15 (100)	9 (82)	0.0797
Positive	9 (27)	0 (0)	2 (18)	
p53				
Abnormal	26 (79)	11 (73)	11 (100)	0.1920
Normal	7 (21)	4 (27)	0 (0)	
p16				
Negative	12 (36)	7 (47)	6 (55)	0.5303
Positive	21 (64)	8 (53)	5 (45)	
SMAD4				
Negative	8 (24)	4 (27)	3 (27)	0.9722
Positive	25 (76)	11 (73)	8 (73)	
β -catenin(membrane)				
loss or weak	10 (30)	8 (53)	8 (73)	0.0347
normal	23 (70)	7 (47)	3 (27)	
DNA sequence				
KRAS				
WT	22 (67)	8 (53)	6 (55)	0.6039
mutation	11 (33)	7 (47)	5 (45)	
BRAF				

WT	32 (97)	15 (100)	10 (91)	0.4424
mutation	1 (3)	0 (0)	1 (9)	

Abbreviations: UICC, Union for International Cancer Control.

Figure 1
(P53)

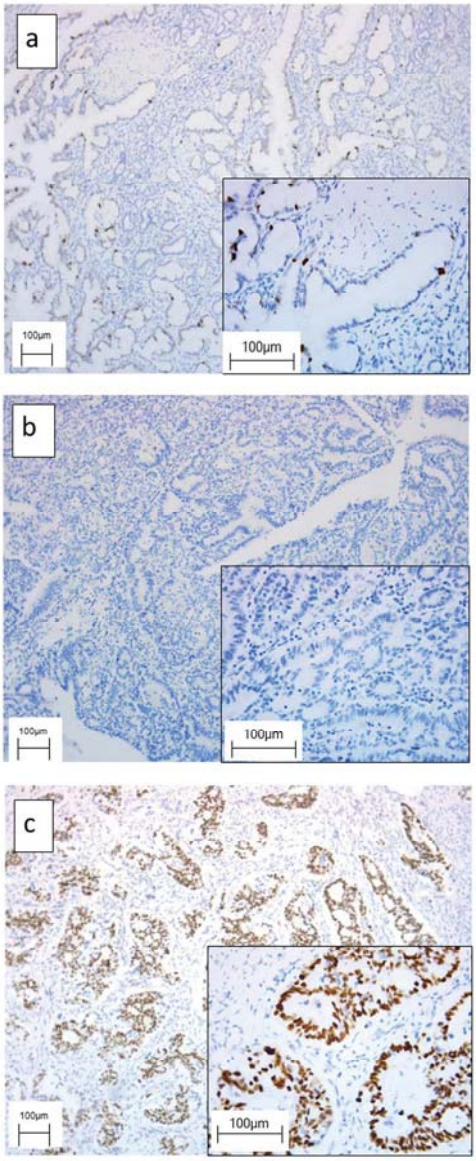

Figure 1
Typical immunohistochemical labeling profiles of p53 in ampullary adenocarcinoma (×100 magnification, lower right×400 magnification). a. (5-30%), Example of normal pattern of ampullary adenocarcinoma for p53. Positive nuclear labeling is present in scattered cells of the neoplastic glands. b. (<5%, loss), Example of abnormal pattern for p53 (loss type). Nuclear labeling is absent in almost every cell of the neoplastic glands. c. (30%<, diffuse), Example of abnormal pattern of p53 (diffuse type). Diffusely positive nuclear labeling is present in the neoplastic glands.

266x355mm (300 x 300 DPI)

Figure 2
(P16)

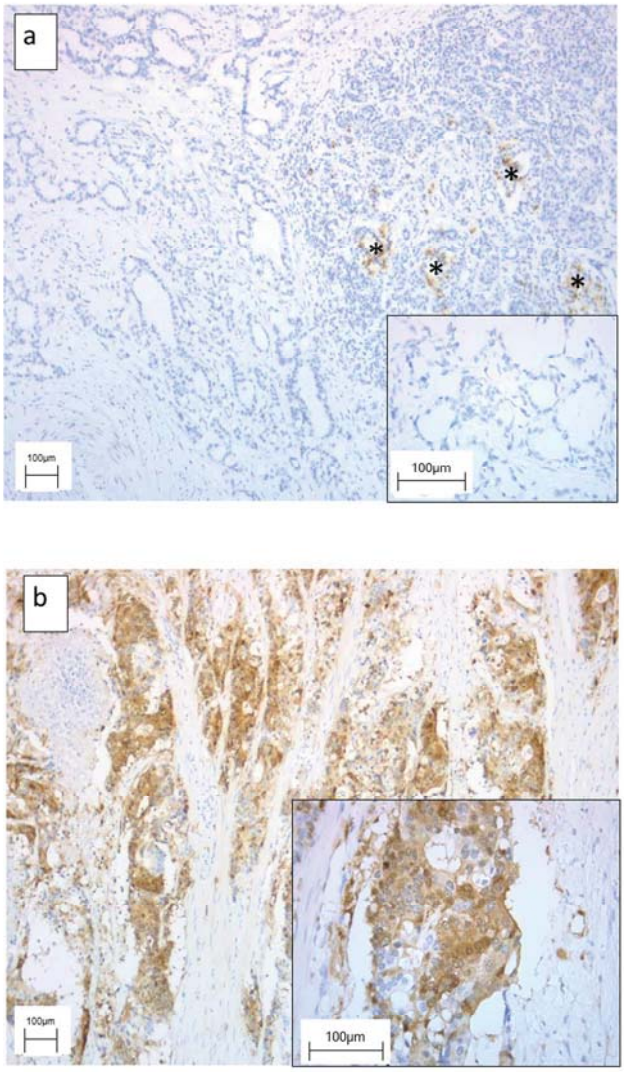

Figure 2
Typical immunohistochemical labeling profiles of p16 in ampullary adenocarcinoma (×100 magnification, lower right×400 magnification). a. Example of negative pattern of ampullary adenocarcinoma for p16. Positive labeling is absent in the neoplastic glands. In contrast, positive labeling is seen within adjacent normal cells (*). b. Example of positive pattern for p16. Positive nuclear and cytoplasmic labeling is present in the neoplastic glands.

266x355mm (300 x 300 DPI)

Figure 3
(Smad4/Dpc4)

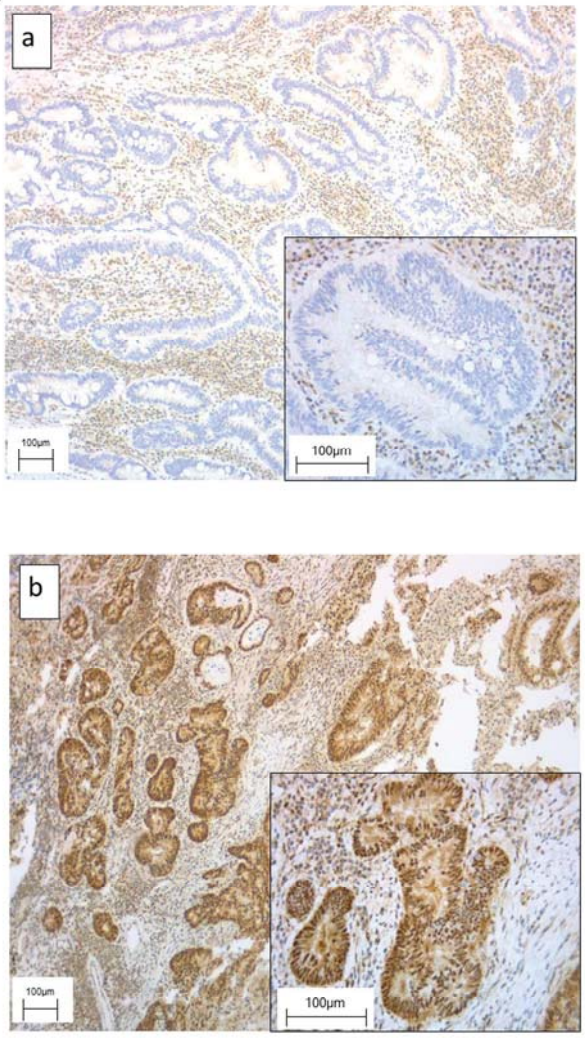

Figure 3
Typical immunohistochemical labeling profiles of Smad4/Dpc4 in ampullary adenocarcinoma (×100 magnification, lower right×400 magnification). a. Example of negative pattern of ampullary adenocarcinoma for Smad4/Dpc4. Nuclear and cytoplasmic labeling is absent in the neoplastic glands. In contrast, positive labeling is seen in adjacent stromal cells. b. Example of positive pattern for Smad4/Dpc4. Positive nuclear and cytoplasmic labeling is present in the neoplastic glands.

266x355mm (300 x 300 DPI)

Figure 4
(beta-catenin)

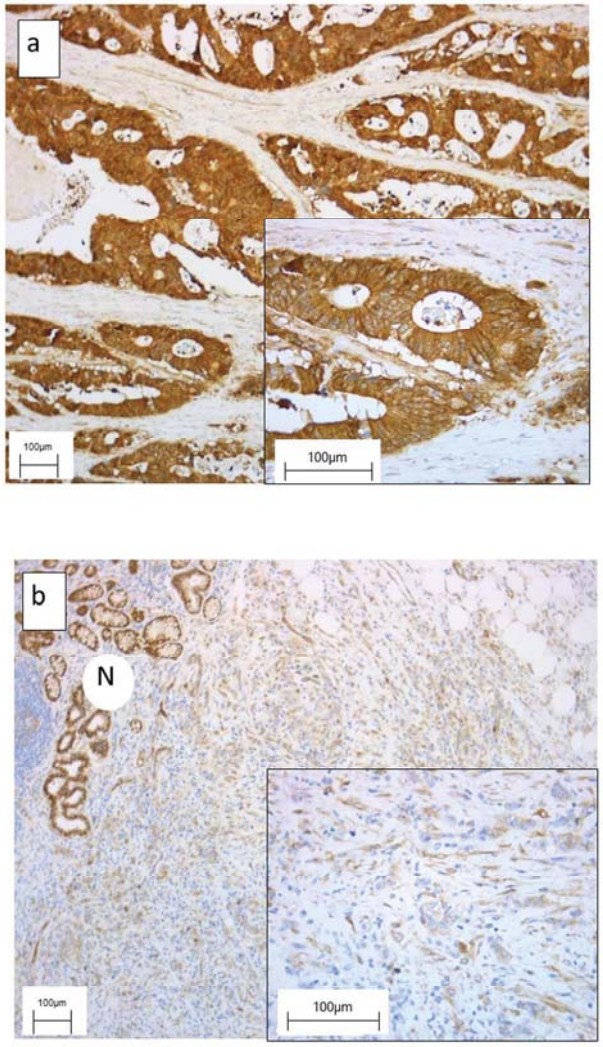

Figure 4
Typical immunohistochemical labeling profiles of β-catenin in ampullary adenocarcinoma (×100 magnification, lower right×400 magnification). a. Example of normal pattern of ampullary adenocarcinoma for β-catenin. Membrane labeling is stronger than nuclear or cytoplasmic labeling in the neoplastic glands. b. Example of loss pattern for β-catenin. Membrane labeling is weak, and positive nuclear or cytoplasmic labeling is present in the neoplastic glands. In contrast, positive membrane labeling is seen in the adjacent normal duodenal glands (N).

266x355mm (300 x 300 DPI)

Figure 5
(MUC1)

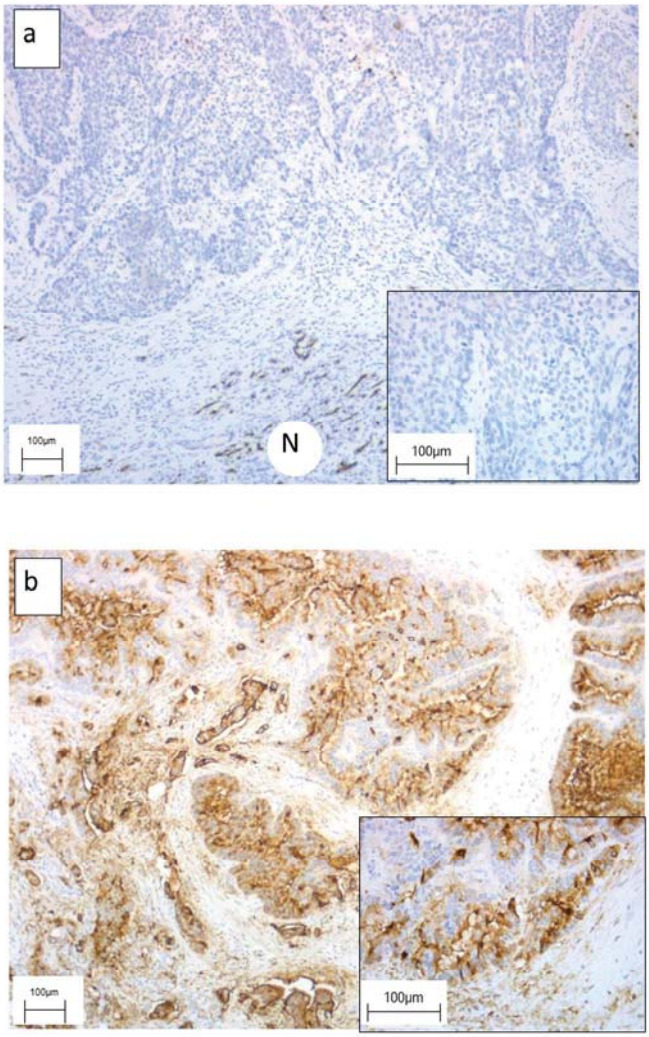

Figure 5
Typical immunohistochemical labeling profiles of MUC1 in ampullary adenocarcinoma (×100 magnification, lower right×400 magnification). a. Example of negative pattern of ampullary adenocarcinoma for MUC1. Positive labeling is absent in the neoplastic glands. In contrast, positive labeling is seen within adjacent normal pancreatic ductal cells (N). b. Example of positive pattern for MUC1. Positive labeling is present in the cytoplasm and membrane of the neoplastic glands.

266x355mm (300 x 300 DPI)

Figure 6
(MUC2)

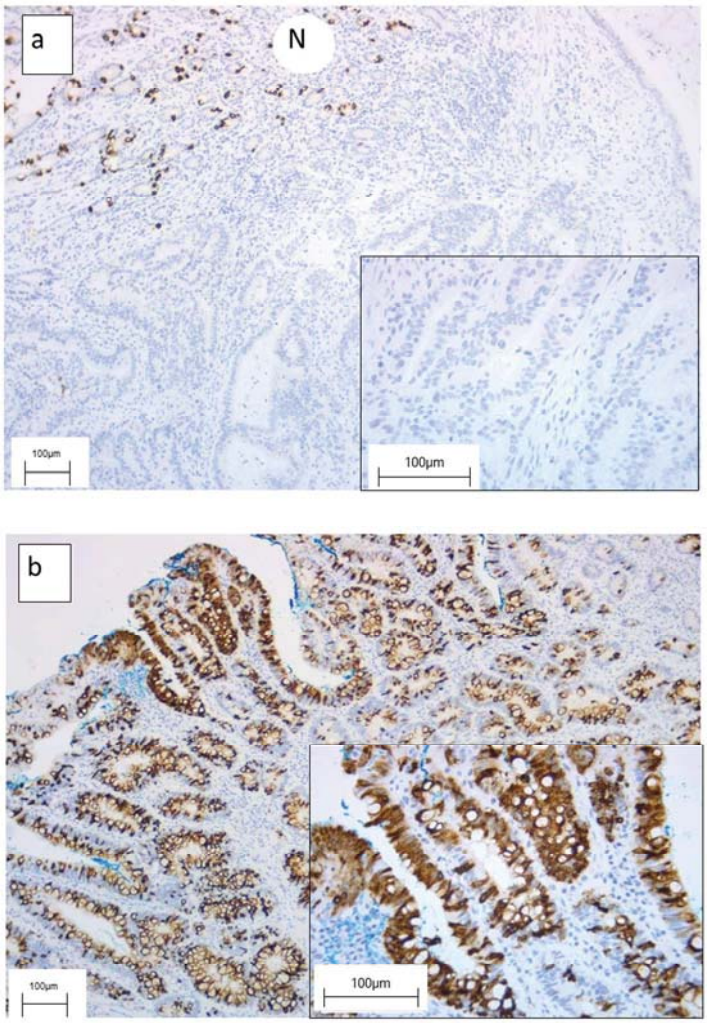

Figure 6
Typical immunohistochemical labeling profiles of MUC2 in ampullary adenocarcinoma (×100 magnification, lower right×400 magnification). a. Example of negative pattern of ampullary adenocarcinoma for MUC2. Positive labeling is absent in the neoplastic glands. In contrast, positive labeling is seen in the goblet cells of adjacent normal duodenal glands (N). b. Example of positive pattern for MUC2. Positive labeling is present in the cytoplasm of the neoplastic glands.

266x355mm (300 x 300 DPI)

Figure 7

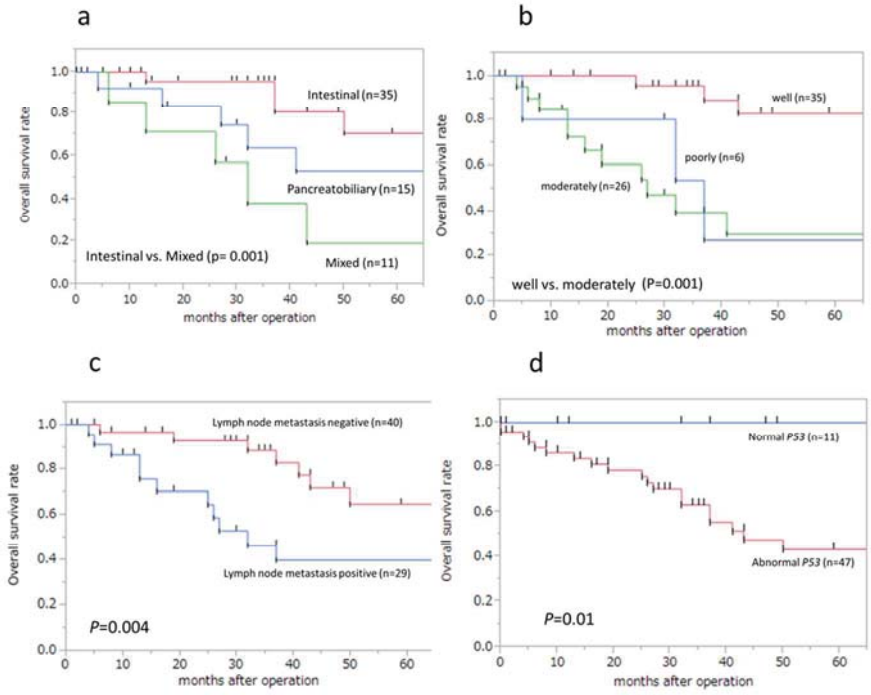

Figure 7
Kaplan-Meier curve of patients with ampullary adenocarcinoma who underwent curative surgery according to the pathologic or immunohistochemical analysis.
a. Subtypes, b. Pathological grade, c. Lymph node metastasis, d. p53 immunolabeling.
The short crossed lines represent the censored cases.

266x355mm (300 x 300 DPI)

Supplementary Table. Clinicopathologic Parameters and molecular biological labeling

Variable	CK20			CK7			CDX2			MUC1			MUC2			p53		
	positive (%)	negative (%)	*P* value	positive (%)	negative (%)	*P* value	positive (%)	negative (%)	*P* value	positive (%)	negative (%)	*P* value	positive (%)	negative (%)	*P* value	Normal (%)	Abnormal (%)	*P* value
Tumor size																		
≤ 20 mm	31 (60)	10 (67)	0.6215	35 (59)	6 (75)	0.3931	13 (50)	28 (68)	0.1343	19 (68)	22 (56)	0.3430	4 (36)	37 (66)	0.0645	10 (83)	31 (56)	0.0824
> 20 mm	21 (40)	5 (33)		24 (41)	2 (25)		13 (50)	13 (32)		9 (32)	17 (44)		7 (64)	19 (34)		2 (17)	24 (44)	
Pathological grade																		
Well	28 (56)	6 (40)	0.4015	30 (53)	4 (50)	0.2350	14 (58)	20 (49)	0.4586	6 (22)	28 (76)	<0.0001	8 (73)	26 (48)	0.2581	7 (59)	27 (51)	0.8978
moderately	17 (34)	8 (53)		23 (40)	2 (25)		7 (29)	18 (44)		20 (71)	5 (13)		3 (27)	22 (41)		4 (33)	21 (40)	
poor	5 (10)	1 (7)		4 (7)	2 (25)		3 (13)	3 (7)		2 (7)	4 (11)		0 (0)	6 (11)		1 (8)	5 (9)	
Lymphatic invasion																		
Negative	19 (40)	3 (21)	0.2116	18 (33)	4 (50)	0.3578	12 (50)	10 (26)	0.0576	4 (15)	18 (51)	0.0028	9 (82)	13 (25)	0.0004	5 (45)	17 (33)	0.4460
Positive	29 (60)	11 (79)		36 (67)	4 (50)		12 (50)	28 (74)		23 (85)	17 (49)		2 (18)	38 (75)		6 (55)	34 (67)	
Vascular invasion																		
Negative	26 (54)	9 (64)	0.5016	31 (57)	4 (50)	0.6933	14 (58)	21 (55)	0.8123	13 (48)	22 (63)	0.2468	9 (82)	26 (51)	0.0614	7 (64)	28 (55)	0.5962
Positive	22 (46)	5 (36)		23 (43)	4 (50)		10 (42)	17 (45)		14 (52)	13 (37)		2 (18)	25 (49)		4 (36)	23 (45)	
Perineural invasion																		
Negative	29 (67)	9 (69)	0.9037	32 (67)	6 (75)	0.6403	14 (61)	24 (73)	0.3499	15 (60)	23 (74)	0.2582	9 (100)	29 (62)	0.0242	5 (63)	33 (69)	0.7260
Positive	14 (33)	4 (31)		16 (33)	2 (25)		9 (39)	9 (27)		10 (40)	8 (26)		0 (0)	18 (38)		3 (37)	15 (31)	
Duodenal invasion																		
Negative	13 (25)	4 (27)	0.8960	16 (27)	1 (12)	0.3726	7 (27)	10 (24)	0.8164	3 (11)	14 (36)	0.0195	5 (45)	12 (21)	0.0941	6 (50)	11 (20)	0.0305

Positive	39 (75)	11 (73)		43 (73)	7 (88)		19 (73)	31 (76)		25 (89)	25 (64)		6 (55)	44 (79)		6 (50)	44 (80)	
Pancreatic invasion																		
Negative	30 (58)	9 (60)	0.8732	36 (61)	3 (37)	0.2057	17 (65)	22 (54)	0.3430	12 (43)	27 (69)	0.0309	10 (91)	29 (52)	0.0162	9 (75)	30 (55)	0.1930
Positive	22 (42)	6 (40)		23 (39)	5 (63)		9 (35)	19 (46)		16 (57)	12 (31)		1 (9)	27 (48)		3 (25)	25 (45)	
Lymph nodes metastasis																		
Negative	31 (60)	8 (53)	0.6639	34 (58)	5 (63)	0.7931	16 (62)	23 (56)	0.6599	10 (36)	29 (74)	0.0016	10 (91)	29 (52)	0.0162	7 (58)	32 (58)	0.9923
Positive	21 (40)	7 (47)		25 (42)	3 (37)		10 (38)	18 (44)		18 (64)	10 (26)		1 (9)	27 (48)		5 (42)	23 (42)	
Stage (UICC)																		
IA	13 (25)	3 (20)	0.5793	15 (26)	1 (12)	0.3919	7 (27)	9 (22)	0.7799	2 (7)	14 (36)	0.0044	5 (45)	11 (20)	0.0420	5 (42)	11 (20)	0.4809
IB	12 (23)	3 (13)		12 (20)	2 (25)		7 (27)	7 (17)		4 (14)	10 (25)		5 (45)	9 (16)		2 (16)	13 (22)	
IIA	5 (10)	1 (7)		4 (7)	2 (25)		2 (8)	4 (10)		2 (7)	4 (10)		0 (0)	6 (11)		0 (0)	6 (11)	
IIB	19 (36)	7 (47)		24 (41)	2 (25)		9 (34)	17 (41)		18 (64)	8 (21)		1 (9)	25 (45)		5 (42)	21 (38)	
III	2 (4)	0 (0)		2 (3)	0 (0)		0 (0)	2 (5)		0 (0)	2 (5)		0 (0)	2 (4)		0 (0)	2 (4)	
IV	1 (2)	2 (13)		2 (3)	1 (12)		1 (4)	2 (5)		2 (7)	1 (3)		0 (0)	3 (5)		0 (0)	3 (5)	

Supplementary Table. (continued) Clinicopathologic Parameters and molecular biological labeling

Variable	p16			Smad4/Dpc4			β - catenin (membrane)			KRAS			BRAF		
	positive (%)	negative (%)	*P* value	positive (%)	negative (%)	*P* value	Normal (%)	loss or weak (%)	*P* value	WT (%)	mutation (%)	*P* value	WT (%)	mutation (%)	*P* value
Tumor size															
≤ 20 mm	17 (46)	24 (80)	0.0044	30 (59)	11 (69)	0.4772	24 (62)	17 (61)	0.9456	29 (73)	11 (42)	0.0142	40 (62)	1 (50)	0.7415
> 20 mm	20 (54)	6 (20)		21 (41)	5 (31)		15 (38)	11 (39)		11 (27)	15 (58)		25 (38)	1 (50)	
Pathological grade															
well	19 (53)	15 (52)	0.9619	25 (51)	9 (56)	0.8726	24 (63)	10 (37)	0.0333	20 (53)	13 (50)	0.3656	34 (54)	0 (0)	0.0878
moderately	14 (39)	11 (38)		19 (39)	6 (38)		13 (34)	12 (44)		13 (34)	12 (46)		24 (38)	1 (50)	
Poor	3 (8)	3 (10)		5 (10)	1 (6)		1 (3)	5 (19)		5 (13)	1 (4)		5 (8)	1 (50)	
Lymphatic invasion															
Negative	14 (42)	8 (28)	0.2231	18 (38)	4 (27)	0.4124	16 (46)	6 (22)	0.0553	14 (36)	7 (32)	0.7475	21 (35)	1 (50)	0.6627
Positive	19 (58)	21 (72)		29 (62)	11 (73)		19 (54)	21 (78)		25 (64)	15 (68)		39 (65)	1 (50)	
Vascular invasion															
Negative	17 (52)	18 (62)	0.4030	27 (57)	8 (53)	0.7797	22 (63)	13 (48)	0.2468	25 (64)	9 (41)	0.0799	33 (55)	2 (100)	0.2067
Positive	16 (48)	11 (38)		20 (43)	7 (47)		13 (37)	14 (52)		14 (36)	13 (59)		27 (45)	0 (0)	
Perineural invasion															
Negative	21 (72)	17 (63)	0.4492	30 (70)	8 (62)	0.5777	22 (69)	16 (67)	0.8688	25 (71)	12 (60)	0.3849	38 (67)	1 (50)	0.3216
Positive	8 (28)	10 (37)		13 (30)	5 (38)		10 (31)	8 (33)		10 (29)	8 (40)		18 (33)	1 (50)	
Duodenal invasion															
Negative	10 (27)	7 (23)	0.7297	14 (27)	3 (19)	0.4853	12 (31)	5 (18)	0.2309	11 (27)	5 (19)	0.4437	17 (26)	0 (0)	0.4025

Positive	27 (73)	23 (77)		37 (73)	13 (81)		27 (69)	23 (82)		29 (73)	21 (81)		48 (74)	2 (100)	
Pancreatic invasion															
Negative	23 (62)	16 (53)	0.4662	32 (63)	7 (44)	0.1789	26 (67)	13 (46)	0.0976	27 (68)	11 (42)	0.0430	37 (57)	2 (100)	0.2238
Positive	14 (38)	14 (47)		19 (37)	9 (56)		13 (33)	15 (54)		13 (32)	15 (58)		28 (43)	0 (0)	
Lymph nodes metastasis															
Negative	21 (57)	18 (60)	0.7890	30 (59)	9 (56)	0.8555	26 (67)	13 (46)	0.0976	22 (55)	16 (62)	0.5995	37 (57)	2 (100)	0.2238
Positive	16 (43)	12 (40)		21 (41)	7 (44)		13 (33)	15 (54)		18 (45)	10 (38)		28 (43)	0 (0)	
Stage (UICC)															
IA	9 (24)	7 (23)	0.8714	13 (25)	3 (19)	0.9153	11 (28)	5 (18)	0.1357	10 (25)	5 (19)	0.8975	16 (25)	0 (0)	0.1674
IB	9 (24)	5 (17)		10 (20)	4 (25)		11 (28)	3 (11)		9 (23)	5 (19)		12 (18)	2 (100)	
IIA	2 (5)	4 (13)		5 (10)	1 (6)		2 (5)	4 (14)		3 (8)	3 (12)		6 (9)	0 (0)	
IIB	14 (38)	12 (40)		20 (39)	6 (38)		12 (31)	14 (50)		16 (40)	10 (38)		26 (40)	0 (0)	
III	1 (3)	1 (3)		1 (2)	1 (6)		2 (5)	0 (0)		1 (2)	1 (4)		2 (3)	0 (0)	
IV	2 (5)	1 (3)		2 (4)	1 (6)		1 (3)	2 (7)		1 (2)	2 (8)		3 (5)	0 (0)	
Abbreviations:UICC, Union for International Cancer Control.															

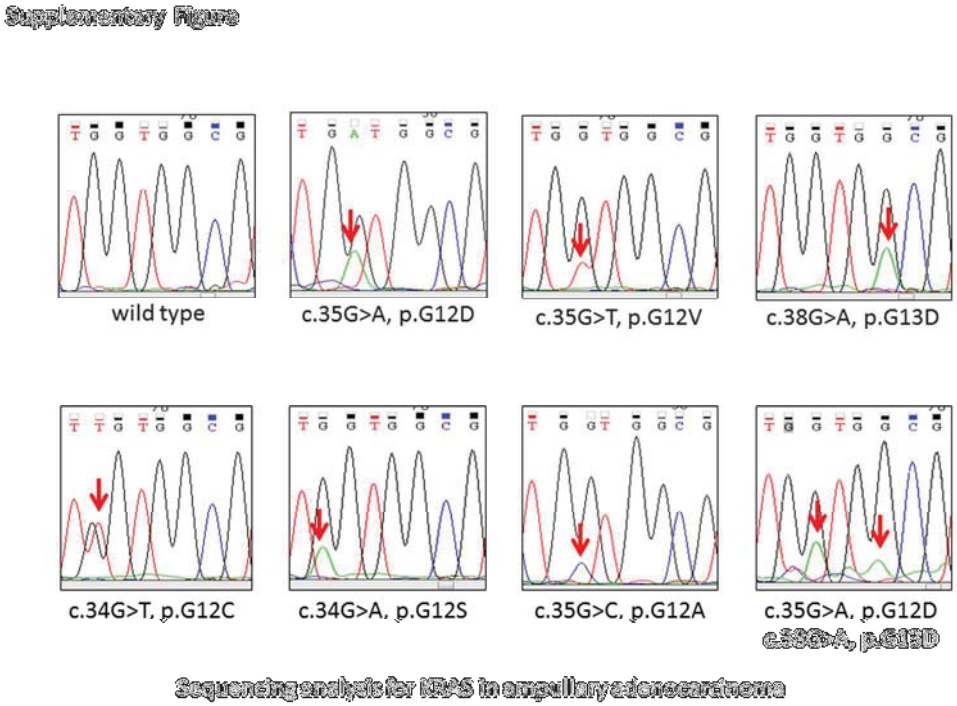

Supplementary Figure
Sequencing analysis of KRAS in ampullary adenocarcinoma.
An activating KRAS gene mutation was identified in 26 of 66 cases of ampullary adenocarcinoma (39.4%). With regard to the amino acid change caused by the KRAS mutation, G12D was detected in 11 cases; G12V was detected in 8 cases; G13D was detected in 3 cases; and G12C, G12S, G12A, and G12D+G13D were detected in 1 case each.

254x190mm (300 x 300 DPI)